

Production of Heavy Quarks in Deep-Inelastic Lepton-Hadron Scattering¹

W.L.van Neerven²

Instituut-Lorentz, Universiteit Leiden, P.O. Box 9506, 2300 RA Leiden, The Netherlands.

Abstract

We will give a review of the computation of exact next-to-leading order corrections to heavy quark production in deep inelastic lepton-hadron scattering and discuss the progress made in this field over the past ten years. In this approach, hereafter called EXACT, where the heavy quark mass is taken to be of the same order of magnitude as the other large scales in the process, one can apply perturbation theory in all orders of the strong coupling constant α_s . The results are compared with another approach, called the *variable flavor number scheme* (VFNS), where the heavy quark is also treated as a massless quark. It turns out that the differences between the two approaches are very small provided both of them are carried out up to next-to-next-to-leading order.

1 Introduction

In the last ten years one has made much progress on the theoretical and experimental level in the study of heavy flavor production in deep inelastic lepton-hadron scattering. Computations of the cross section in the Born approximation, where the heavy quark is treated as a massive particle, were finished by the end of the seventies [1] whereas the first experimental results came from the EMC-collaboration [2] in the early eighties. In the nineties the $\mathcal{O}(\alpha_s)$ corrections to the Born process were computed in [3]. Moreover other methods to study heavy flavor production were advocated like the intrinsic quark approach [4] and the variable flavor number scheme [5] where the heavy quark is also treated as a massless particle. From the experimental side the electron (positron)-proton collider HERA has given us a wealth of information about charm quark production (for recent experimental results see [6], [7], [8], [9]). We will report about this progress below.

The semi-inclusive process describing heavy quark production in deep inelastic electron-proton scattering is given by (see Fig. 1)

$$e^-(k_1) + P(p) \rightarrow e^-(k_2) + Q(p_1) + X', \quad (1)$$

¹Talk presented at the Mignerone Tribute Session of the conference MRST 2001, The University of Western Ontario, London, Canada, May 15-18

²Work supported by the EC network 'QCD and Particle Structure' under contract No. FMRX-CT98-0194.

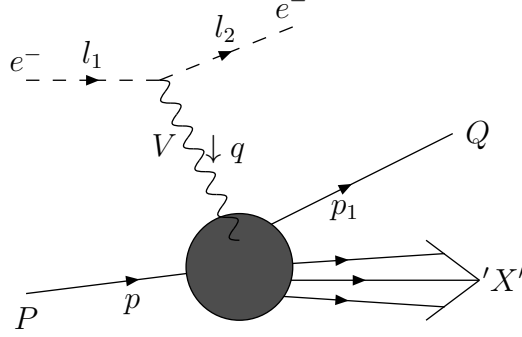


Figure 1: Kinematics of heavy quark Q -production in deep inelastic electron-proton scattering

where V represents the intermediate vector boson Z or γ carrying the momentum q and Q denotes the heavy (anti-) quark. The scaling variables are given by

$$x = \frac{Q^2}{2p \cdot q}, \quad y = \frac{p \cdot q}{p \cdot k_1},$$

$$q^2 = (k_1 - k_2)^2 \equiv -Q^2 < 0, \quad 0 < x \leq 1, \quad 0 < y < 1. \quad (2)$$

In the ongoing experiments carried out at HERA [6], [7], [8], [9] and in the fixed target experiments carried out in the past [2], $Q^2 \ll M_Z^2$ so that the intermediate Z -boson can be neglected and the reaction is dominated by photon exchange. In this case the inclusive cross section simplifies considerably and when the incoming particles are unpolarised it can be written as

$$\frac{d^2\sigma}{dx dQ^2} = \frac{2\pi\alpha^2}{xQ^4} \left[\left\{ 1 + (1-y)^2 \right\} F_{2,Q}(x, Q^2, m^2) - y^2 F_{L,Q}(x, Q^2, m^2) \right], \quad (3)$$

where $F_{k,Q}$ ($k = 2, L$) denote the heavy quark contributions to the structure functions. Notice that an analogous formula exists for the semi-inclusive cross section

$$\frac{d^4\sigma}{dx dy dp_{T,Q} d\eta_Q}, \quad (4)$$

where $p_{T,Q}$ and η_Q denote the transverse momentum and rapidity of the heavy quark Q respectively. Both of them are considered in the center of mass of the photon-proton system. For neutral current reactions one has proposed two different production mechanisms for heavy quark production. They are distinguished as follows

I Intrinsic Heavy Quark Production

Here one assumes that, besides light quarks u, d, s and gluons g , the wave function of the proton also consists of heavy quarks like c, b, t [4]. In the context of the QCD improved parton model this means that the production mechanism is described as indicated in Fig. 2. In this picture the heavy quark emerges directly from the proton and interacts with the virtual photon γ^* . The consequence is that it is described by a heavy flavor density $f_Q(z, \mu^2)$ with $p_Q = zp$ and μ denotes the factorization scale. For this mechanism the

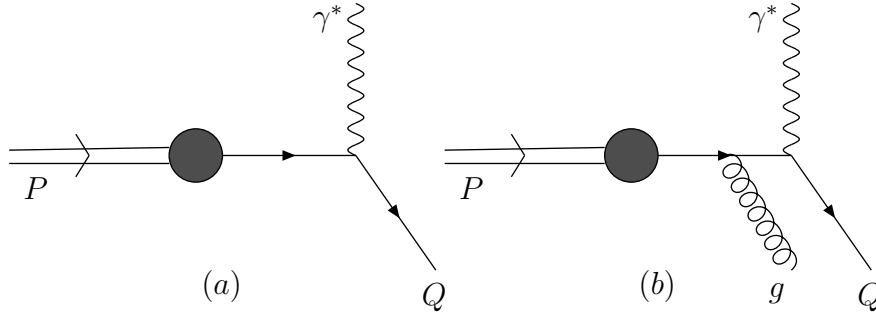


Figure 2: (a) $\gamma^* + Q \rightarrow Q$ ($H_{k,Q}^{(0)}$), (b) $\gamma^* + Q \rightarrow Q + g$ ($H_{k,Q}^{(1)}$).

heavy quark structure function has the following representation

$$\begin{aligned}
 F_{k,Q}(x, Q^2, m^2) &= e_Q^2 \int_x^1 \frac{dz}{z} f_Q(x/z, \mu^2) H_{k,Q}(z, Q^2, m^2, \mu^2) \\
 &\equiv e_Q^2 f_Q(\mu^2) \otimes H_{k,Q}(Q^2, m^2, \mu^2).
 \end{aligned} \tag{5}$$

Here e_Q denotes the charge of the heavy quark and \otimes stands for the convolution

$$f \otimes g(x) = \int_x^1 \frac{dz}{z} f(x/z) g(z). \tag{6}$$

Further the heavy quark coefficient function $H_{k,Q}$ can be expanded in the strong coupling constant $\alpha_s(\mu^2)$ as follows

$$H_{k,Q} = \sum_{n=0}^{\infty} a_s^n H_{k,Q}^{(n)}, \quad \text{with} \quad a_s \equiv \frac{\alpha_s}{4\pi}. \tag{7}$$

Some of the contributions to $H_{k,Q}$ are given by the diagrams in Fig. 2a,b.

II Extrinsic Heavy Quark Production

In this case the proton wave function does not contain the heavy quark components. In lowest order of perturbation theory the heavy quark and heavy anti-quark appear in pairs and are produced via photon-gluon fusion [1] as presented in Fig. 3. Here the gluon emerges from the proton in a similar way as the heavy quark in Fig. 2. In this approach the heavy quark structure function reads in lowest order

$$F_{k,Q}(x, Q^2, m^2) = a_s e_Q^2 f_g(\mu^2) \otimes H_{k,g}^{(1)}(Q^2, m^2, \mu^2). \tag{8}$$

The main difference between the two production mechanisms can be attributed to the fact that for extrinsic heavy quark production two heavy particles are produced in the final state instead of one as in the case of the intrinsic heavy quark approach. This reveals itself in the transverse momentum p_T -distribution where for mechanism II the quark and anti-quark appear back to back. The experiments carried out HERA [9] confirm the p_T -spectrum predicted by the latter

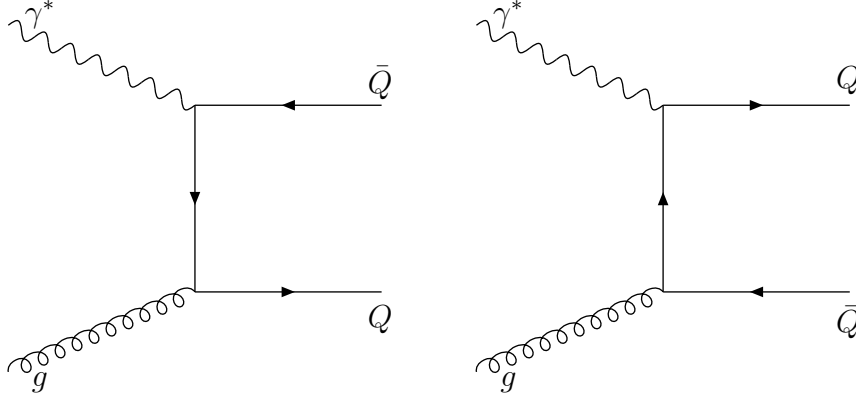


Figure 3: Feynman diagrams for the lowest-order photon-gluon fusion process contributing to the coefficient functions $H_{k,g}^{(1)}$.

mechanism. However in the past the EMC-collaboration [2] found a discrepancy at large x ($x = 0.237$) between the structure function $F_{2,Q}$, predicted by mechanism II, and the charm quark data. This difference can be explained by also invoking mechanism I [4] (see also [10]). Nevertheless because of the success of extrinsic heavy quark production revealed by the HERA charm quark data we will continue with this approach in our calculations below.

2 Heavy Quark Structure Functions up to $\mathcal{O}(\alpha_s^2)$

In the extrinsic heavy quark approach there are two different production mechanisms [11], [12] which are of importance for the derivation of the variable flavor number scheme (VFNS) treated in the next section. In the case of electro-production the virtual photon either interacts with the heavy quark appearing in the final state or it is attached to the light (anti-) quark in the initial state. This distinction is revealed by the Feynman graphs. Some of them will be shown as illustration below.

A The photon interacts with the heavy quark

Here the lowest order (LO) process is given by gluon fusion as presented in Fig. 3. It is given by the partonic reaction

$$\gamma^* + g \rightarrow Q + \bar{Q}, \quad (9)$$

which is calculated in [1]. In next-to-leading order (NLO) one has to compute the virtual corrections to this process. Some of the Feynman graphs are shown in Fig. 4. Besides the virtual corrections one also has to calculate all processes which contain an extra particle in the final state. Adding a gluon to reaction (9) we observe gluon bremsstrahlung given by

$$\gamma^* + g \rightarrow Q + \bar{Q} + g. \quad (10)$$

Some of the Feynman graphs corresponding to the process above are presented in Fig. 5. Besides this reaction we have another one which appears for the first time if the computations are extended to NLO. It is represented by the Bethe-Heitler process

$$\gamma^* + q(\bar{q}) \rightarrow Q + \bar{Q} + q(\bar{q}), \quad (11)$$

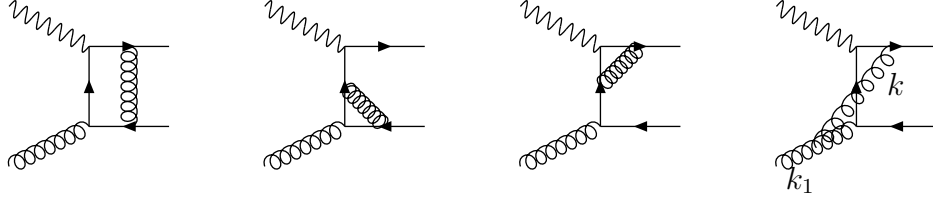


Figure 4: Virtual gluon corrections to the process $\gamma^* + g \rightarrow Q + \bar{Q}$ contributing to the coefficient functions $H_{i,g}^{(2)}$.

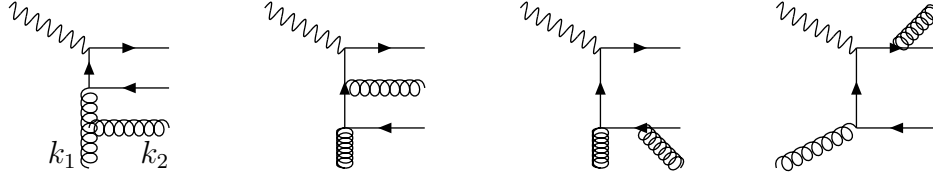


Figure 5: The bremsstrahlung process $\gamma^* + g \rightarrow Q + \bar{Q} + g$ contributing to the coefficient functions $H_{i,g}^{(2)}$.

where the Feynman diagrams are shown in Fig. 6. The contributions to the heavy quark structure functions due to the reactions above can be written as

$$\begin{aligned}
 F_{k,Q}(Q^2, m^2) = & e_Q^2 \left[f_g(3, \mu^2) \otimes \left\{ a_s(\mu^2) H_{k,g}^{(1)}(Q^2, m^2) + a_s^2(\mu^2) H_{k,g}^{(2)}(Q^2, m^2, \mu^2) \right\} \right. \\
 & \left. + a_s^2(\mu^2) f_q^S(3, \mu^2) \otimes H_{k,q}^{(2)}(Q^2, m^2, \mu^2) \right]. \quad (12)
 \end{aligned}$$

Here e_Q denotes the charge of Q indicating that the photon couples to the heavy quark and $H_{k,i}$ ($i = g, q$), characteristic of these type of processes, represent the heavy quark coefficient functions which emerge from the calculation of the Feynman graphs after renormalization and mass factorization is carried out. The former procedure leads to a dependence on a renormalization scale μ of the coupling constant a_s , the coefficient function $H_{k,i}$ and the parton densities f_i . Moreover the latter two also depend on a factorization scale which

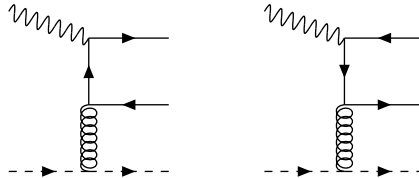


Figure 6: The Bethe-Heitler process $\gamma^* + Q \rightarrow Q + \bar{Q} + q$ contributing to the coefficient functions $H_{i,q}^{(2)}$.



Figure 7: The Compton process $\gamma^* + Q \rightarrow Q + \bar{Q} + q$ contributing to the coefficient functions $L_{i,q}^{(2)}$.

for convenience is set equal to the parameter μ defined above. The factorization scale, which can be attributed to mass factorization, appears in all coefficient functions except for the lowest order one i.e. $H_{k,i}^{(1)}$. In the structure function of Eq. (12) there appear two different types of flavor singlet parton densities i.e. the gluon density f_g and the quark singlet density which in a three flavor number scheme reads as

$$f_q^S(3, \mu^2) = f_u(3, \mu^2) + f_{\bar{u}}(3, \mu^2) + f_d(3, \mu^2) + f_{\bar{d}}(3, \mu^2) + f_s(3, \mu^2) + f_{\bar{s}}(3, \mu^2). \quad (13)$$

Hence Eq. (12) represents the singlet part of the heavy quark structure function.

B The photon interacts with the light quark.

The second production mechanism is represented by the Feynman diagrams where the photon couples to the light quark or the anti-quark. This happens for the first time in NLO where one observes the Compton process

$$\gamma^* + q(\bar{q}) \rightarrow Q + \bar{Q} + q(\bar{q}), \quad (14)$$

which is depicted in Fig. 7. The coefficient functions corresponding to this type of process are denoted by $L_{k,i}$ ($i = q, g$) and the contribution to the heavy quark structure functions is characterized by the expression

$$F_{k,Q}(Q^2, m^2) = \sum_{i=u,d,s} e_i^2 a_s^2(\mu^2) \left(f_i(3, \mu^2) + f_{\bar{i}}(3, \mu^2) \right) \otimes L_{k,q}^{(2)}(Q^2, m^2), \quad (15)$$

where e_i denotes the charge of the light quark represented by $i = u, d, s$ in a three flavor number scheme. Since this process appears for the first time in second order mass factorization is not needed which explains the independence of $L_{k,q}^{(2)}$ on the parameter μ .

The computation of the second order contributions to the heavy quark coefficient functions $H_{k,i}$, $L_{k,i}$ has been carried out in [3]. While calculating the Feynman graphs in Figs. 4- 6 one encounters several type of singularities which have to be regularized and subsequently to be subtracted off before one obtains a finite result. The singularities are of the following nature i.e. infrared (IR), ultraviolet (UV) and collinear (C). Sometimes the latter are also called mass singularities. The IR divergences cancel between the virtual and the bremsstrahlung corrections to reaction (9). The UV divergences, regularized by n-dimensional regularization, are removed by mass and coupling constant renormalization. For the mass renormalization we choose the

on-shell scheme. In this case the UV divergence will be removed by replacing the bare mass \hat{m} by the renormalized mass m via

$$\hat{m} = m \left[1 + \hat{a}_s \delta_0 \frac{2}{\varepsilon} + \dots \right], \quad (16)$$

where the UV pole term is indicated by $1/\varepsilon$ with $\varepsilon = n - 4$. If we choose for example process (10) together with the virtual corrections to the Born reaction (9) (see Figs. 4,5) the unrenormalized coefficient function takes the form

$$\begin{aligned} \hat{H}_{k,g}^{(2)} &= \hat{a}_s^2 \left[\left\{ \frac{1}{\varepsilon_C} + \frac{1}{2} \ln \left(\frac{m^2}{\mu^2} \right) \right\} P_{gg}^{(0)} \otimes H_{k,g}^{(1)} - \beta_0 \left\{ \frac{2}{\varepsilon_{UV}} + \ln \left(\frac{m^2}{\mu^2} \right) \right\} H_{k,g}^{(1)} \right] \\ &+ H_{k,g}^{(2)}|_{\mu=m}, \end{aligned} \quad (17)$$

where $H_{k,g}^{(2)}|_{\mu=m}$ is finite and \hat{a}_s denotes the bare coupling constant. Further we have also regularized the collinear divergences by n -dimensional regularization. In order to distinguish between ultraviolet and collinear divergences we have indicated them by $1/\varepsilon_{UV}$ and $1/\varepsilon_C$ respectively. The residues of the collinear divergences are represented by the so called splitting functions denoted by P_{ij} ($i, j = q, g$). The origin of the collinear divergences is explained by the first diagram in Fig. 5. The propagator carrying the momentum $k_1 - k_2$ behaves as

$$\frac{1}{(k_1 - k_2)^2} = \frac{1}{2\omega_1\omega_2(1 - \cos\theta)}, \quad (18)$$

which diverges for $\theta \rightarrow 0$. This propagator only shows up if three massless particles are coupled to each other like three gluons or when a gluon is attached to a quark line provided the quark is massless. If the gluon is attached to a heavy quark the mass of the latter, which is unequal to zero, prevents that the denominator in Eq. (18) vanishes when $\theta \rightarrow 0$. The UV-divergence in Eq. (17) is removed by coupling constant renormalization which is achieved by adding $\hat{a}_s H_{k,g}^{(1)}$ to Eq. (17) and replacing the bare coupling constant \hat{a}_s by the renormalized one represented by $a_s(\mu^2)$

$$\hat{a}_s = a_s(\mu^2) \left[1 + a_s(\mu^2) \beta_0 \frac{2}{\varepsilon} + \dots \right]. \quad (19)$$

Finally one has to remove the collinear divergences. This is achieved by mass factorization. It proceeds in a similar way as multiplicative renormalization so that one can write

$$\hat{H}_{k,i} \left(\frac{1}{\varepsilon_C}, Q^2, m^2 \right) = \Gamma_{ji} \left(\frac{1}{\varepsilon_C}, \mu^2 \right) \otimes H_{k,j} \left(Q^2, m^2, \mu^2 \right), \quad (20)$$

where Γ_{ji} represents the transition function which removes all collinear divergences from the bare heavy quark coefficient functions. Further we have introduced the notion of bare parton density \hat{f}_i so that the heavy quark structure function can be written as

$$F_{k,Q}(Q^2, m^2) = e_Q^2 \hat{f}_i \otimes \hat{H}_{k,i} \left(\frac{1}{\varepsilon_C}, Q^2, m^2 \right). \quad (21)$$

Substitution of $\hat{H}_{k,i}$ (see Eq. (20)) into the expression above we can derive

$$F_{k,Q}(Q^2, m^2) = e_Q^2 f_j(\mu^2) \otimes H_{k,j} \left(Q^2, m^2, \mu^2 \right), \quad (22)$$

where $f_j(\mu^2)$ is the renormalized parton density defined by

$$f_j(\mu^2) = \Gamma_{ji} \left(\frac{1}{\varepsilon_C}, \mu^2 \right) \otimes \hat{f}_i. \quad (23)$$

In the case of the example presented in Eq. (18) the collinear divergence is removed by adding $H_{k,g}^{(1)}$ to $\hat{H}_{k,g}^{(2)}$ and choosing the following transition function

$$\Gamma_{gg} \left(\frac{1}{\varepsilon_C}, \mu^2 \right) = \delta(1-z) + a_s N \left[\frac{1}{\varepsilon_C} P_{gg}^{(0)} \right], \quad (24)$$

where N denotes the number of colors.

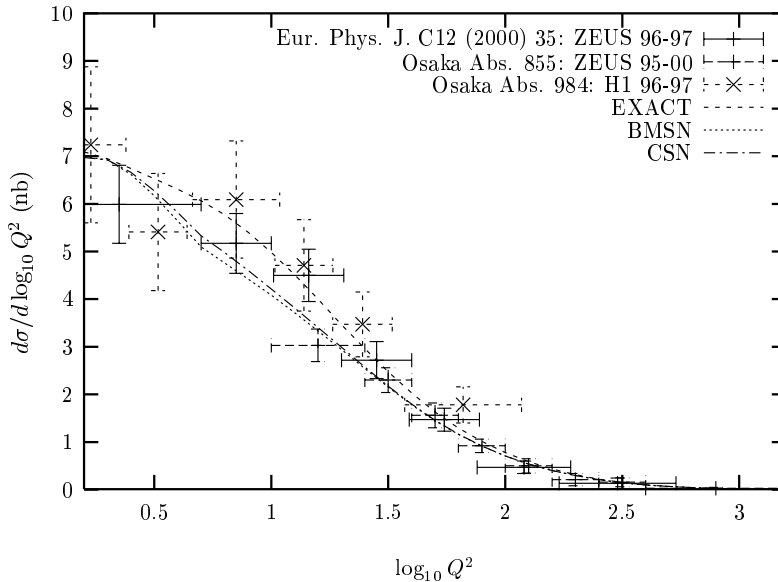


Figure 8: The combined Osaka and published Zeus-data for $d\sigma/d\log_{10}Q^2$ in nb for deep inelastic production of $D^{*\pm}$ -mesons. The dashed line is the exact NLO result from the program HVQDIS which follows from $F_{2,c}^{\text{EXACT}}$. The dotted line (BMSN-scheme) and dashed-dotted line (CSN-scheme) is based on $F_{2,c}^{\text{VFNS}}$.

A comparison of the next-to-leading order (NLO) heavy quark structure function $F_{2,c}$ with the data for charm quark production measured at HERA reveals a fairly good agreement between theory and experiment. The data cover the range $1 < Q^2 < 1350 \text{ GeV}^2$ and $5 \times 10^{-5} < x < 5.6 \times 10^{-2}$. In [13] one has made a comparison with the data obtained by the ZEUS-collaboration [6], [8]. From the cross section in Eq. (2) one can derive the integrated quantities

$$\frac{d\sigma}{dQ^2} = \int_{x_{\min}}^{x_{\max}} dx \frac{d^2\sigma}{dx dQ^2}, \quad \frac{d\sigma}{dx} = \int_{Q_{\min}^2}^{Q_{\max}^2} dQ^2 \frac{d^2\sigma}{dx dQ^2}. \quad (25)$$

Notice that the quantities above represent D_c^* -meson production rather than charm quark production. The meson appears as a fragmentation product of the quark and the cross sections in Eq. (25) are obtained by convoluting Eq. (2) with fragmentation functions. Furthermore one has to impose experimental cuts on the kinematics which are indicated by max and min . The results are presented in Figs. 8, 9 which originate from [13] where one can also find the maximal and minimal values for x and Q^2 . The figures show that there is a good agreement between the exact NLO result (called EXACT in the figure) and the data except for $x \sim 10^{-3}$ where there is a small discrepancy. Furthermore in [14] one has also made a comparison between the program HQVDIS [15] based on the NLO computations above and the experimental differential distributions for D_c^* production where the following cross sections are studied.

$$\frac{d\sigma}{dp_{T,D_c}}, \quad \frac{d\sigma}{d\eta_{D_c}}, \quad \frac{d\sigma}{dW}, \quad (26)$$

where W ($W^2 = (p + q)^2$) is the center of mass energy of the photon-proton system. Also the differential distributions agree with the NLO predictions except for the rapidity η -distribution. Here it appears that for $\eta_D > 0$ the experimental cross section is larger than the one computed in NLO (see also [9]).

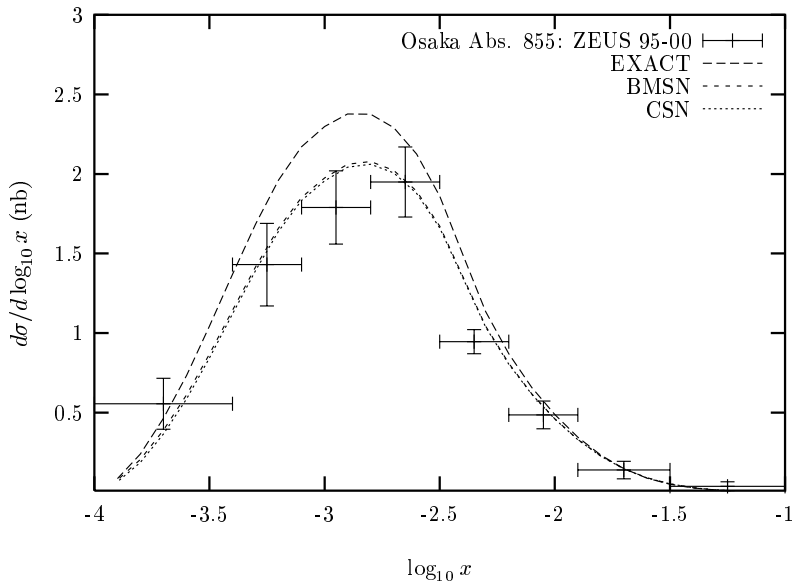


Figure 9: The combined Osaka and published Zeus-data for $d\sigma/d\log_{10}x$ in nb for deep inelastic production of $D^{*\pm}$ -mesons. The dashed line is the exact NLO result from the program HQVDIS which follows from $F_{2,c}^{\text{EXACT}}$. The dotted line (BMSN-scheme) and dashed-dotted line (CSN-scheme) is based on $F_{2,c}^{\text{VFNS}}$.

Summarizing our findings for the exact NLO calculations we conclude

1. There exist a fairly good agreement between the data and the NLO calculations.

2. The theoretical curves are insensitive to the choice of the renormalization/factorization scale μ occurring in the parton densities and the coefficient functions [16].
3. The theoretical curves are sensitive to the choice of the charm mass m_c which is in the range $1.3 < m_c < 1.7 \text{ GeV}/c^2$.
4. Processes with a gluon in the initial state (Eqs. (9),(10)) constitute the bulk of the contribution to the heavy quark structure function at $x < 10^{-2}$. Hence they are an excellent probe to measure the gluon density $f_g(z, \mu^2)$.

3 Asymptotic Heavy Quark Structure Functions

In this section we want to study the heavy quark coefficient functions $H_{k,i}, L_{k,i}$ in the asymptotic region $Q^2 \gg m^2$. In this region they have the following form

$$H_{k,i}^{\text{ASYMP}}(z, Q^2, m^2, \mu^2) \sim \sum_{l=1}^{\infty} a_s^l \sum_{n+m \leq l} a_{nm}(z) \ln^n \left(\frac{\mu^2}{m^2} \right) \ln^m \left(\frac{Q^2}{m^2} \right). \quad (27)$$

A similar expression exists for $L_{k,i}^{\text{ASYMP}}$. An example is the asymptotic expression for the Born reaction in Eq. (9) (Fig. 3) which can be written as

$$H_{2,g}^{\text{ASYMP}}(z, Q^2, m^2) = a_s \left[\frac{1}{2} P_{qg}(z) \ln \left(\frac{Q^2}{m^2} \right) + a_{Qg}(z) + c_{2,g}(z) \right]. \quad (28)$$

The origin of this asymptotic behaviour can be attributed to the property that in the limit $m \rightarrow 0$ the heavy quark coefficient functions become collinear divergent which is revealed by the logarithmic singularities $\ln Q^2/m^2$ and $\ln \mu^2/m^2$. The reason why this behaviour is of interest can be summarized as follows

1. The results obtained for the exact coefficient functions in the previous section are semi-analytic. In [3] one has obtained exact results for the virtual corrections to process (9) (Fig. 4) but for the reactions with three particles in the final state like Eqs. (10),(11), (14) a full analytical expression could only be presented for the Compton process in Eq. (14) (see [11]). In the other cases only the integration over the angles could be carried out but the integration over the final state energies are so tedious that they have to be done in a numerical way. However the latter integration becomes more amenable when $m^2 \ll Q^2$ so that terms of the order m^2/Q^2 can be neglected. Therefore an analytical result for the asymptotic heavy quark coefficient functions provides us with a check of the exact expressions computed for arbitrary m .
2. The asymptotic coefficient functions play an important role in the derivation of the variable flavor number scheme [5], [17] discussed at the end of this section. This scheme is only useful if the following questions are answered. They are:
 - a. Do the logarithmic terms of the type $\ln^n Q^2/m^2$, occurring in the coefficient functions, really dominate the heavy quark structure functions or the heavy quark cross sections?
 - b. Are the logarithmic terms $\ln^n Q^2/m^2$ so large that they bedevil the perturbation series so that they have to be re-summed?

There are two ways to compute the asymptotic heavy quark coefficient functions.

1. One can follow the procedure for the derivation of the exact coefficient functions in [3] but since the mass m can be neglected one can now carry out the additional integrations over the energies of the final state particles in an analytical way.
2. One can use the operator product expansion (OPE) techniques which however are only applicable for inclusive quantities like the structure functions $F_{k,Q}(x, Q^2, m^2)$.

In [11] one has adopted the latter approach which will be outlined below. In the derivation of the cross section in Eq. (3) one encounters the hadronic tensor leading to the definition of the structure functions. It is defined by

$$\begin{aligned}
W_{\mu\nu}(p, q) &= \frac{1}{4\pi} \int d^4z e^{iq \cdot z} \langle P(p) | [J_\mu(z), J_\nu(0)] | P(p) \rangle \\
&= \left(p_\mu p_\nu - \frac{p \cdot q}{q^2} (p_\mu q_\nu + p_\nu q_\mu) + g_{\mu\nu} \frac{(p \cdot q)^2}{q^2} \right) \frac{F_2(x, Q^2, M^2)}{p \cdot q} \\
&+ \left(g_{\mu\nu} - \frac{q_\mu q_\nu}{q^2} \right) \frac{F_L(x, Q^2, M^2)}{2x}, \\
p^2 &= M^2, \quad q^2 = -Q^2, \quad x = \frac{Q^2}{2p \cdot q}.
\end{aligned} \tag{29}$$

In the limit $Q^2 \gg M^2$ the current-current correlation function appearing in the integrand of Eq. (29) is dominated by the light cone. Hence one can make an operator product expansion near the light cone and write

$$\left[J(z), J(0) \right] \underset{z^2 \rightarrow 0}{\sim} \sum_i \sum_m c_i^{(m)}(z^2, \mu^2) z_{\mu_1} \cdots z_{\mu_m} O_i^{\mu_1 \cdots \mu_m}(0, \mu^2), \tag{30}$$

where for convenience we have dropped the Lorentz indices of the currents. Here $c_i^{(m)}$ denote the coefficient functions which are distributions and $O_i^{\mu_1 \cdots \mu_m}$ are local operators. Both are renormalized which is indicated by the renormalization scale μ . When dropping all terms of the order M^2/Q^2 we can limit ourselves to leading twist operators. In QCD they are given by

non-singlet operators

$$O_{q,r}^{\mu_1 \cdots \mu_m}(z) = \frac{1}{2} i^{m-1} \mathcal{S} \left[\bar{\psi}(z) \gamma^{\mu_1} D^{\mu_2} \cdots D^{\mu_m} \frac{\lambda_r}{2} \psi(z) \right] + \text{trace terms},$$

singlet operators

$$O_q^{\mu_1 \cdots \mu_m}(z) = \frac{1}{2} i^{m-1} \mathcal{S} \left[\bar{\psi}(z) \gamma^{\mu_1} D^{\mu_2} \cdots D^{\mu_m} \psi(z) \right] + \text{trace terms},$$

$$O_g^{\mu_1 \cdots \mu_m}(z) = \frac{1}{2} i^{m-2} \mathcal{S} \left[F_\alpha^{a, \mu_1}(z) D^{\mu_2} \cdots D^{\mu_{m-1}} F_\alpha^{a, \mu_m}(z) \right] + \text{trace terms}. \tag{31}$$

The symbol \mathcal{S} indicates that one has to symmetrize over all Lorentz indices. The covariant derivative is given by $D^\mu = \partial^\mu - i g T_a A_a^\mu$ and λ_r is the generator of the flavor group $SU(n_f)_F$. Insertion of the OPE (Eq. (30)) into the hadronic tensor of Eq. (29) leads to the following result

$$F_k^{(m)}(Q^2, M^2) \equiv \int_0^1 dx x^{m-1} F(x, Q^2) = \sum_{i=q,g} A_i^{(m)} \left(\frac{\mu^2}{M^2} \right) C_i^{(m)} \left(\frac{Q^2}{\mu^2} \right), \tag{32}$$

where the operator matrix element and the coefficient function are defined by

$$A_i^{(m)} \left(\frac{\mu^2}{M^2} \right) = \langle P(p) | O_i^m(0, \mu^2) | P(p) \rangle, \quad C_i^{(m)} \left(\frac{Q^2}{\mu^2} \right) = \int d^4 z e^{iq \cdot z} c_i^{(m)}(z^2 \mu^2). \quad (33)$$

The OPE techniques can also be applied when the the proton state $|P(p)\rangle$ in Eq. (29) is replaced by a light quark state $|q(p)\rangle$ or a gluon state $|g(p)\rangle$. However when the proton is replaced by massless quarks and gluons the external momentum satisfies the relation $p^2 = 0$ so that the partonic structure functions and the partonic operator matrix elements become collinearly divergent. One can show (see [17]) that instead of Eq. (32) one obtains more complicate expressions which are given by

$$\begin{aligned} & \hat{\mathcal{F}}_{k,q}^{\text{NS}} \left(\frac{Q^2}{\mu^2}, \frac{1}{\varepsilon_C} \right) + \hat{L}_{k,q}^{\text{ASYMP}} \left(\frac{Q^2}{m^2}, \frac{m^2}{\mu^2}, \frac{1}{\varepsilon_C} \right) = \hat{A}_{qq}^{\text{NS}} \left(\frac{m^2}{\mu^2}, \frac{1}{\varepsilon_C} \right) \otimes \mathcal{C}_{k,q}^{\text{NS}} \left(\frac{Q^2}{\mu^2} \right), \\ & \hat{\mathcal{F}}_{k,i}^{\text{S}} \left(\frac{Q^2}{\mu^2}, \frac{1}{\varepsilon_C} \right) + \hat{L}_{k,i}^{\text{ASYMP}} \left(\frac{Q^2}{m^2}, \frac{m^2}{\mu^2}, \frac{1}{\varepsilon_C} \right) + \hat{H}_{k,i}^{\text{ASYMP}} \left(\frac{Q^2}{m^2}, \frac{m^2}{\mu^2}, \frac{1}{\varepsilon_C} \right) \\ & = \hat{A}_{ji}^{\text{S}} \left(\frac{m^2}{\mu^2}, \frac{1}{\varepsilon_C} \right) \otimes \mathcal{C}_{k,j}^{\text{NS}} \left(\frac{Q^2}{\mu^2} \right), \\ & i, j = q, g. \end{aligned} \quad (34)$$

Here $\hat{\mathcal{F}}_{k,i}$ represent the partonic structure functions which are given by Feynman graphs containing massless particles only and therefore contain collinear singularities indicated by ε_C . These singularities also appear in the asymptotic heavy quark coefficient functions $\hat{H}_{k,i}^{\text{ASYMP}}$, $\hat{L}_{k,i}^{\text{ASYMP}}$ which are determined in the asymptotic regime $Q^2 \gg m^2$ before mass factorization is carried out. These collinear divergences can be traced back to the massless quarks and gluons appearing in Figs. 3-7. Finally \hat{A}_{ji} represent the operator matrix elements on the partonic level and are defined by

$$\hat{A}_{ji} \left(\frac{m^2}{\mu^2}, \frac{1}{\varepsilon_C} \right) = \langle i | O_j(\mu^2, 0) | i \rangle, \quad i = q, g, \quad j = q, g, Q, \quad p_i^2 = 0. \quad (35)$$

The operator matrix elements which depend on the heavy flavor mass consist of two classes. The first class is given by heavy quark operators sandwiched between gluon or light quark states. The second class contains light quark or gluon operators which contain a heavy flavor loop. Examples of the first class together with the corresponding process are given in Figs. 10 and 11. An example of the second class is shown in 12. The light partonic coefficient functions defined by $\mathcal{C}_{k,j}$ are derived from the light partonic structure functions via mass factorization

$$\hat{\mathcal{F}}_{k,i} \left(\frac{Q^2}{\mu^2}, \frac{1}{\varepsilon_C} \right) = \Gamma_{ji} \left(\frac{1}{\varepsilon_C}, \mu^2 \right) \otimes \mathcal{C}_{k,j} \left(\frac{Q^2}{\mu^2} \right), \quad (36)$$

where Γ_{ji} denote the transition functions which are discussed below Eq. (20). The quantities $\hat{\mathcal{F}}_{k,i}$ and $\mathcal{C}_{k,i}$ have been calculated up to second order in α_s in [18]. The operator matrix elements \hat{A}_{ij} are also known up to second order and the calculation of them is presented in [11], [17]. Like in the case of the coefficient functions n-dimensional regularization has been used to regularize the ultraviolet and collinear divergences and one has chosen the same renormalization conditions

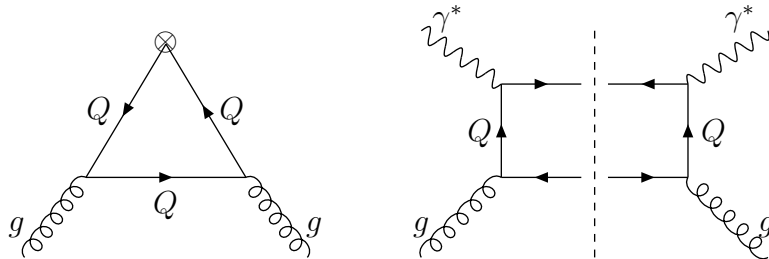


Figure 10: The operator matrix element $A_{Qg}^{(1)}$ and the corresponding Feynman graph for the process $\gamma^* + g \rightarrow Q + \bar{Q}$ ($H_{k,g}^{(1)}$).

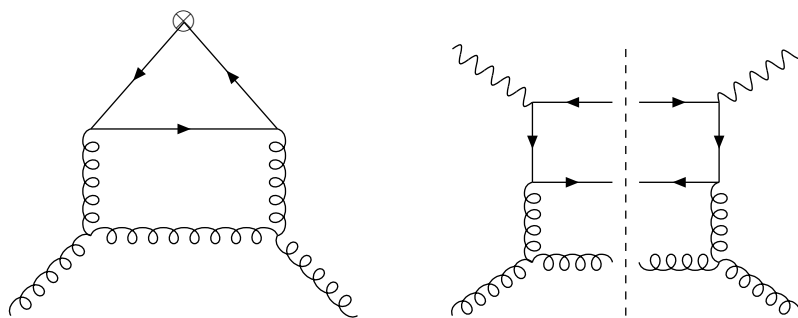


Figure 11: The operator matrix element $A_{Qg}^{(2)}$ and the corresponding Feynman graph for the process $\gamma^* + g \rightarrow Q + \bar{Q} + g$ ($H_{k,g}^{(2)}$).

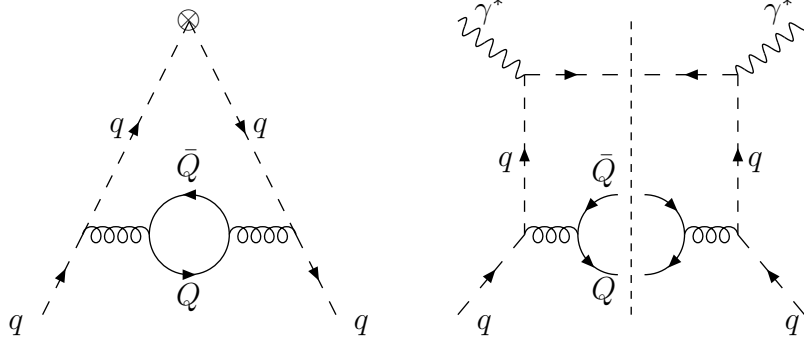


Figure 12: The operator matrix element $A_{qq}^{\text{NS},(2)}$ and the corresponding Feynman graph for the process $\gamma^* + q \rightarrow Q + \bar{Q} + q$ ($L_{k,q}^{\text{NS},(2)}$).

for the mass and the strong coupling constant. Hence from Eq. (34) one infers the asymptotic heavy quark coefficient functions $\hat{H}_{k,i}^{\text{ASYMP}}$, $\hat{L}_{k,i}^{\text{ASYMP}}$ up to the same order (see [17]). Finally one can remove the remaining collinear divergences via the same mass factorization as is done for the exact heavy quark coefficient functions in Eq. (20). After this outline of the calculation of the asymptotic heavy quark coefficient function one might ask the question whether it is not easier to compute them in a more direct way. The main problem of radiative corrections is the computation of the phase space integrals in particular if one has massive particles in the final state even if one takes $m^2 \ll Q^2$. Since this work was already done for the light partonic structure functions $\hat{\mathcal{F}}_{k,i}$ in [18] it was not needed to repeat this procedure anymore. On the contrary it is much easier to compute two-loop operator matrix elements because of the zero momentum flowing into the operator vertex indicated by the symbol \otimes in Figs. 10-12. The difference between the exact and asymptotic coefficient functions can be attributed to the power corrections of the type $(m^2/Q^2)^l$, with $l \geq 1$, which occur in the former but are absent in the latter. The asymptotic coefficient functions only contain the logarithms $\ln^m Q^2/m^2$ and $\ln^n \mu^2/m^2$ and terms which survive in the limit $Q^2 \rightarrow \infty$. We will now first answer the question whether these logarithmic terms dominate the heavy quark structure function $F_{k,Q}(x, Q^2, m^2)$. For that purpose we have studied the structure functions for charm production i.e. $Q = c$ in [17], [19]. Here one has computed the ratio

$$R_{k,c} = \frac{F_{k,c}^{\text{ASYMP}}}{F_{k,c}^{\text{EXACT}}}, \quad (37)$$

where $F_{k,c}^{\text{EXACT}}$ and $F_{k,c}^{\text{ASYMP}}$ are represented in the three flavor number scheme

$$F_{k,c}^{\text{EXACT}} = \frac{4}{9} \sum_{i=q,g} f_i^{\text{S}}(3, \mu^2) \otimes H_{k,i}^{\text{EXACT}} + \sum_{j=u,d,s} e_j^2 (f_j(3, \mu^2) + f_j(3, \mu^2)) \otimes L_{k,q}^{\text{EXACT}}, \quad (38)$$

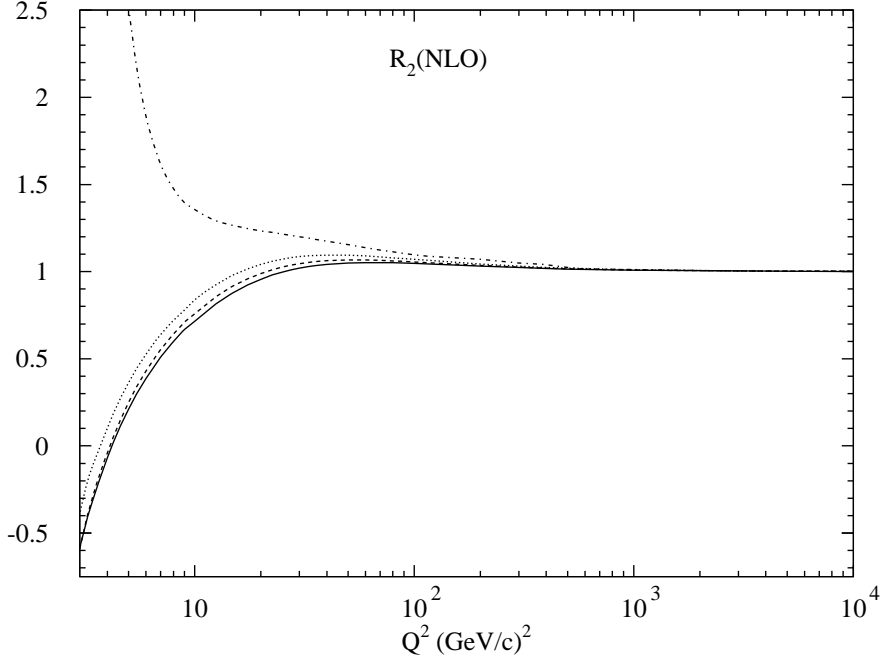


Figure 13: $R_{2,c}$ in NLO (Eq. (37)) plotted as function of Q^2 at fixed x ; $x = 10^{-1}$ (dashed-dotted line), $x = 10^{-2}$ (dotted line), $x = 10^{-3}$ (dashed line), $x = 10^{-4}$ (solid line) .

$$\begin{aligned}
F_{k,c}^{\text{ASYMP}} = & \\
& \frac{4}{9} \sum_{i=q,g} f_i^S(3, \mu^2) \otimes H_{k,i}^{\text{ASYMP}} + \sum_{j=u,d,s} e_j^2 (f_j(3, \mu^2) + f_{\bar{j}}(3, \mu^2)) \otimes L_{k,q}^{\text{ASYMP}} .
\end{aligned} \tag{39}$$

In Fig. 13 we have plotted $R_{2,c}$. Here one observes that this quantity becomes very close to one for $x < 10^{-2}$ and $Q^2 > 20 \text{ GeV}^2$ which belongs to the region explored by the experiments carried out at HERA. This shows that the logarithms mentioned above dominate the structure function except in the threshold region given by $x \sim 1$ and small Q^2 which is characteristic of the EMC experiment [2].

In order to answer the second question whether these logarithmic terms vitiate the perturbation series one has to resum them in all orders of perturbation theory and show that the resummed structure function differs from the one which is computed exactly in fixed order of perturbation theory. This resummation procedure is provided by the variable flavor number scheme (VFNS) [5]. An example of a resummed structure function has been derived in [17]. In the case of charm quark production one obtains

$$F_{k,c}^{\text{VFNS}} = \sum_{j=u,d,s,c} e_j^2 \left[(f_j(4, \mu^2) + f_{\bar{j}}(4, \mu^2)) \otimes \mathcal{C}_{k,j}^{\text{VFNS}} + f_g(4, \mu^2) \otimes \mathcal{C}_{k,g}^{\text{VFNS}} \right], \tag{40}$$

with the conditions

$$\lim_{m^2 \rightarrow 0} \mathcal{C}_{k,i}^{\text{VFNS}} \left(\frac{Q^2}{m^2}, \frac{\mu^2}{m^2} \right) = \mathcal{C}_{k,i} \left(\frac{Q^2}{\mu^2} \right), \quad (41)$$

$$\lim_{s \rightarrow 4m^2} F_{k,c}^{\text{VFNS}}(x, Q^2, m^2) = F_{k,c}^{\text{EXACT}}(x, Q^2, m^2), \quad s = \frac{1-x}{x} Q^2. \quad (42)$$

The consequence of condition (41) is that in the asymptotic regime $Q^2 \gg m^2$, $F_{k,c}^{\text{VFNS}}$ turns into the structure function represented in the four flavor number scheme which contains the contribution of light flavors only including the charm quark. The mass singular logarithms, occurring in the heavy quark coefficient functions in the three flavor number scheme (see Eqs. (12), (15)), are shifted to the parton densities defined in the four flavor number scheme appearing in Eq. (40). The most conspicuous feature is the appearance of the charm quark density which is absent in a three flavor number scheme but shows up in the four flavor number scheme. It is given by

$$f_c(4, \mu^2) + f_{\bar{c}}(4, \mu^2) = f_q^{\text{S}}(3, \mu^2) \otimes A_{Qq}^{\text{S}} \left(\frac{\mu^2}{m^2} \right) + f_g(3, \mu^2) \otimes A_{Qg}^{\text{S}} \left(\frac{\mu^2}{m^2} \right). \quad (43)$$

The operator matrix elements satisfy renormalization group equations which enable us to resum all logarithmic terms of the type $\ln \mu^2/m^2$. In order to get the boundary condition (42) one needs matching conditions for which one can make various choices (see e.g. [5], [17], [20]). Two of them are proposed in [17],[21] (BMSN scheme) and in [22] (CSN scheme). In the former one equates

$$\mathcal{C}_{k,c}^{\text{VFNS}} \left(\frac{Q^2}{m^2}, \frac{\mu^2}{m^2} \right) = \mathcal{C}_{k,q} \left(\frac{Q^2}{\mu^2} \right), \quad q = u, d, s. \quad (44)$$

Both schemes have been calculated up to next-to-next-to-leading order (NNLO) and are compared in [13] with $F_{k,c}^{\text{EXACT}}$ (NLO) in Eq. (38). The results are shown in Figs. 8, 9 from which one infers that there is hardly any difference between the two schemes representing VFNS. This shows that one can neglect the power contributions $\mathcal{O}(m^2/Q^2)$ in $\mathcal{C}_{k,c}^{\text{VFNS}}$ which are absent in $\mathcal{C}_{k,q}$. Also the difference between the two versions of VFNS on one hand and the exact NLO approach on the other hand is hardly noticeable except in Fig. 9 where in the vicinity of $x = 10^{-3}$ it seems that the data are better described by the BMSN and CSN schemes than by the exact NLO result. The main conclusion that one can draw from these figures is that the resummation effect is very small which means that the so called large logarithms of the type $\ln Q^2/m^2$ and also $\ln \mu^2/m^2$, when $\mu^2 \sim Q^2$, do not vitiate the perturbation series.

Summarizing our results we conclude

1. The past ten years have shown much progress in the computation of higher order corrections to heavy flavor production. In particular the results obtained in electro-production agree well with the data obtained by the experiments carried out at HERA.
2. The asymptotic heavy quark coefficient functions can be calculated using operator product expansion techniques. The results obtained for the operator matrix elements can be also used for processes where the light cone does not dominate the reaction which e.g. holds for $e^+ e^- \rightarrow \mu^+ \mu^-$ [23].

3. The heavy quark structure function is dominated by the logarithmic terms $\ln Q^2/m^2$ and $\ln \mu^2/m^2$ provided x and Q^2 are chosen in such a way that they are outside the threshold region of the production process i.e.
 $s = (1 - x)Q^2/x \gg 4m^2$.
4. In spite of the fact that the logarithms above dominate the structure function they do not bedevil the convergence of the perturbation series so that a resummation is in principle not necessary. Therefore one can use fixed order (exact) perturbation theory which is simple to apply and to interpret in particular if one studies the differential distributions presented in Eqs. (4), (26).

References

- [1] Witten E., *Nucl. Phys.* **B104**, 445 (1976);
 Babcock J. and Sivers D., *Phys. Rev.* **D18**, 2301 (1978);
 Shifman M.A., Vainstein A.I. and Zakharov V.J., *Nucl. Phys.* **B136**, 157 (1978);
 Glück M. and Reya E., *Phys. Lett.* **B83** 98 (1978);
 Leveille J.V. and Weiler T., *Nucl. Phys.* **B147**, 147 (1979).
- [2] Aubert J.J. et al., (EMC-collaboration), *Nucl. Phys.* **B213**, 31 (1983).
- [3] Laenen E, Riemersma S., Smith J. and van Neerven W.L., *Nucl. Phys.* **B392**, 162 (1993);
 ibid. *Nucl. Phys.* **B392** 229 (1993);
 Riemersma S., Smith J and van Neerven W.L., *Phys. Lett.* **B347**, 43 (1995).
- [4] Brodsky S.J., Hoyer P., Mueller A.H., Tang W.-K., *Nucl. Phys.* **B369** 519 (1992);
 Vogt R., Brodsky S.J., *Nucl. Phys.* **B438** 261 (1995).
- [5] Aivazis M.A.G., Collins J.C., Olness F.I. and W. -K. Tung, *Phys. Rev.* **D50**, 3102 (1994).
- [6] Breitweg J. et al. (ZEUS-collaboration), *Eur. Phys. J.* **C12**, 35 (2000).
- [7] Adloff C. et al. (H1-collaboration), *Nucl. Phys.* **B545**, 21 (1999).
- [8] ZEUS-collaboration, Abstract 855, submitted to the *XXXth International Conference on High Energy Physics*, July 27-August 2, 2000, Osaka, Japan.
- [9] H1-collaboration, Abstract 984, submitted to the *XXXth International Conference on High Energy Physics*, July 27-August 2, 2000, Osaka, Japan.
- [10] Harris B.W., Smith J, Vogt R., *Nucl. Phys.* **B461**, 181 (1996).
- [11] Buza M., Matiounine Y., Smith J., Mignerone R., van Neerven W.L., *Nucl. Phys.* **B472**, 611 (1996); ibid. *Nucl. Phys. Proc. Suppl.* **51C**, 183 (1996).
- [12] van Neerven W.L. , *Acta Phys. Polon.* **B28**, 2715 (1997), hep-ph/9708452.
- [13] Chuvakin A, Smith J. and Harris B.W., *Eur. Phys. J.* **C18**, 547 (2001).
- [14] Harris B.W., Smith J., *Phys. Rev.* **D57**, 2806 (1998).

- [15] Harris B.W. and Smith J., *Nucl. Phys.* **B452** 109 (1995); *ibid. Nucl. Phys. Proc. Suppl* **51C** 188-194 (1996), hep-ph/9605358.
- [16] Glück M, Reya E., Stratmann M., *Nucl. Phys.* **B222** 37 (1994); Vogt A., hep-ph/9601352, Proceedings of *Deep Inelastic Scattering and Related Phenomena "DIS96"*. Editors 'Agostini G.D. and Nigro A., (World Scientific), p. 254.
- [17] Buza. M, Matiounine Y., Smith J. and van Neerven W.L., *Eur. Phys. J.* **C1**, 301 (1998); *ibid. Phys. Lett.* **B411**, 211 (1997).
- [18] van Neerven W.L. and Zijlstra E.B., *Phys. Lett.* **B272**, 127 (1991); Zijlstra E.B. and van Neerven W.L., *Phys. Lett.* **B273**, 476 (1991); Zijlstra E.B. and van Neerven W.L., *Nucl. Phys.* **B383**, 525 (1992).
- [19] Laenen E. et al., hep-ph/9609351, Published in the proceedings of the *Workshop on Future Physics at HERA*, Hamburg, Germany, 25-26 Sep 1995, p. 393-401.
- [20] Thorne R.S. and Roberts R.G., *Phys. Lett.* **B421**, 303 (1998); *ibid. Phys. Rev.* **D57**, 6871 (1998).
- [21] van Neerven W.L. , hep-ph/9804445, Published in the Proceedings of the *6th International Workshop on Deep Inelastic Scattering and QCD "DIS98"*, Editors Coremans GH. and Roosen R., World Scientific, p. 162-166.
- [22] Chuvakin A, Smith J. and van Neerven W.L., *Phys. Rev.* **D61**, 096004 (1999), *ibid. Phys. Rev.* **D62**, 036004 (2000).
- [23] Berends F.A., van Neerven W.L., Burgers G.J.H., *Nucl. Phys.* **B297**, 429 (1988); Erratum: *Nucl. Phys.* **B304**, 921 (1988).